

# Deuterium/tritium behavior in Flibe and Flibe-facing materials

R.A. Anderl<sup>a,\*</sup>, S. Fukada<sup>b</sup>, G.R. Smolik<sup>a</sup>, R.J. Pawelko<sup>a</sup>, S.T. Schuetz<sup>a</sup>,  
J.P. Sharpe<sup>a</sup>, B.J. Merrill<sup>a</sup>, D.A. Petti<sup>a</sup>, H. Nishimura<sup>c</sup>, T. Terai<sup>c</sup>, S. Tanaka<sup>c</sup>

<sup>a</sup> Idaho National Engineering and Environmental Laboratory (INEEL), P.O. Box 1625, Idaho Falls, ID, 83415, USA

<sup>b</sup> Kyushu University, Hakozaki, Higashi-ku, Fukuoka 812-8581, Japan

<sup>c</sup> The University of Tokyo, Hongo, Bunkyo-ku, Tokyo 113-8656, Japan

## Abstract

Experimental studies to investigate the behavior of deuterium and tritium in the molten salt Flibe ( $2\text{LiF} \cdot \text{BeF}_2$ ), have been conducted as part of the Japan–US joint research program (JUPITER-II). Measurements of deuterium transport were made in a cylindrically symmetric, dual permeation probe assembly containing 400 cc of Flibe. An exact analytical transport solution in cylindrical coordinates was fit to the measured permeation data, and this analysis derived deuterium diffusion and solubility coefficients of  $8.0 \times 10^{-10} \text{ m}^2/\text{s}$  and  $3.1 \times 10^{-4} \text{ mol/m}^3 \text{ Pa}$  at 600 °C, respectively, and  $3.0 \times 10^{-9} \text{ m}^2/\text{s}$  and  $1.0 \times 10^{-4} \text{ mol/m}^3 \text{ Pa}$  at 650 °C. The diffusion coefficients were about a factor of two less than previous results derived from capillary-reservoir diffusion measurements with tritium. Solubility results were significantly greater than previously measured for  $\text{D}_2$  but they were comparable to those for DF in Flibe. The results suggest that the dominant deuterium transport species in Flibe was  $\text{D}^+\text{F}^-$  for these experiments.

© 2004 Elsevier B.V. All rights reserved.

## 1. Introduction

The fluoride salt,  $2\text{LiF} \cdot \text{BeF}_2$ , commonly referred to as Flibe, has been proposed for use in self-cooled tritium breeder blankets for inertial and magnetic fusion applications [1–3]. Tritium recovery and permeation losses and structural material corrosion are key issues that impact the successful implementation of molten Flibe for such use. Neutron transmutation reactions in Flibe produce the desired tritium but also generate free or excess fluorine that can affect tritium behavior in the molten salt and enhance material corrosion if not managed properly with suitable REDOX (reduction-oxidation) control [4]. In recent years, a joint collaborative research effort has been established as part of the second Japan–US Program on Irradiation Tests for Fusion Energy Research (JUPITER-II) to address the tritium chemistry and corrosion control issues for the

molten salt breeder blanket [5]. The purpose of this paper is to report the results of initial JUPITER-II experiments that investigated the transport behavior of deuterium in molten Flibe in an effort to better understand diffusion and solution properties of hydrogen isotopes in Flibe.

Tritium behavior in molten salts depends strongly on the tritium chemical species in the salt and on the diffusive and solution properties of those species [6]. Several experiments focused on characterization of tritium species in Flibe under neutron exposure [7–11]. These experiments indicated that the tritium was borne as  $\text{T}^+$  and most likely bonded to  $\text{F}^-$  in the salt as TF, unless there was an abundance of hydrogen in solution. Use of hydrogen in purge gas streams over and through the molten salt increased the solution hydrogen, promoted changes in the tritium chemical species to HT via exchange reactions, enhanced release of tritium from the salt to the gas phase above the salt, and enhanced tritium permeation through metal walls surrounding the molten salt. Only a few studies reported diffusion and solution properties. Diffusion coefficients (500–800 °C) were derived in experiments based on  $\text{T}^+$  diffusion from

\* Corresponding author. Tel.: +1-208 533 4153; fax: +1-208 533 4207.

E-mail address: [raa@inel.gov](mailto:raa@inel.gov) (R.A. Anderl).

a capillary containing irradiated Flibe into a reservoir containing molten Flibe [12]. Tritium diffusion as  $T^+$  was also measured for solid Flibe at temperatures from 350 to 400 °C [13]. Solubility measurements, made for  $H_2$ ,  $D_2$ , HF and DF in Flibe at 500–700 °C, indicated that the solubility of  $H_2$  and  $D_2$  was about a factor of 100 less than that for HF and DF at 600 °C [14,15].

## 2. Experimental details

### 2.1. Permeation probe setup

Deuterium transport experiments were conducted in a cylindrically symmetric, dual probe permeation pot setup illustrated in Fig. 1. The assembly consisted of a type-316 stainless-steel pot, a nickel crucible for containing Flibe, two permeation probes of thin-walled nickel, a gas-manifold to enable Ar purge gas flow through assembly volumes, and a quadrupole mass spectrometer (QMS) for on-line measurements of the flow stream gas compositions. Each probe was equipped with barrier volumes at the top to minimize direct deuterium transport between the probes and the cover gas above the molten salt. Typically, with the pot at test temperature, probe-1 was pressurized with deuterium to about 0.9 atm and QMS analysis of Ar gas from probe-2 provided a measure of the deuterium that permeated through the walls of probe-1, the molten Flibe and the walls of probe-2. The barrier volumes and the volumes above the salt were purged with separate Ar gas streams that were analyzed sequentially with the QMS. Standard gas mixtures containing  $H_2$  in Ar and  $D_2$  in Ar were used to calibrate the on-line QMS so that deuterium partial pressures could be derived from the measured

data. A nitrogen-purged glove box housed the permeation pot assembly and associated heater.

The permeation probe assembly was designed and fabricated with cylindrical symmetry to facilitate one-dimensional model simulation and analysis of deuterium transport in the system. Nickel was selected as the Flibe-facing material because it is corrosion-resistant in the molten salt environment and its hydrogen permeability is more than 1000 times faster than that for Flibe. Overall dimensions of the steel pot were: 178 mm height and a 102 mm OD pot wall that was 3 mm thick. Nickel crucible dimensions were: 91.4 mm OD, 85 mm ID and 150 mm height. Probe-2 was a cylindrical annulus with 75 mm OD, 51 mm ID, 0.5 mm wall, and 110 mm height. Probe-1 was a 12 mm OD cylinder with 0.5 mm wall and a 110 mm height.

### 2.2. Flibe preparation

Approximately 400 cc of Flibe were used in the permeation probe experiment. This material was prepared from reagent-grade LiF and  $BeF_2$  that was previously degassed in an inert furnace at 250 °C, combined in a 2:1 ratio and heated at 600 °C. Chemical purification of the Flibe was done by a hydro-fluorination process in which molten Flibe was purged with a gas stream containing HF and  $H_2$  in a 1:10 ratio to facilitate reduction of oxide impurities in the melt [16]. Chemical analysis of the processed Flibe identified oxygen and carbon impurities at 600 and 45 ppm in the purified product. A heated transfer line, equipped with a porous stainless steel filter (60 micron pore) to block solid-phase impurity material transfer, was used to transfer molten Flibe from the supply pot to the permeation pot. Transfer of 400 cc of Flibe filled the permeation pot to a level to ensure that any deuterium observed in probe-2 originated via transport through Flibe.

## 3. Measurements, analysis and results

### 3.1. Permeation measurements without Flibe

Prior to experiments with Flibe, the permeation probe assembly was conditioned and tested at temperatures up to 700 °C. The purpose of these tests was to ensure leak tightness of the dual probe assembly during thermal cycling, to verify the performance of the gas-handling system and the QMS analysis approach, and to benchmark deuterium transport model calculations for the assembly against measured deuterium permeation data. The results of these experiments and model calculations were described in detail in previous publications [17,18]. Derived permeability values from these experiments were in excellent agreement with previously published hydrogen diffusivity and solubility data for

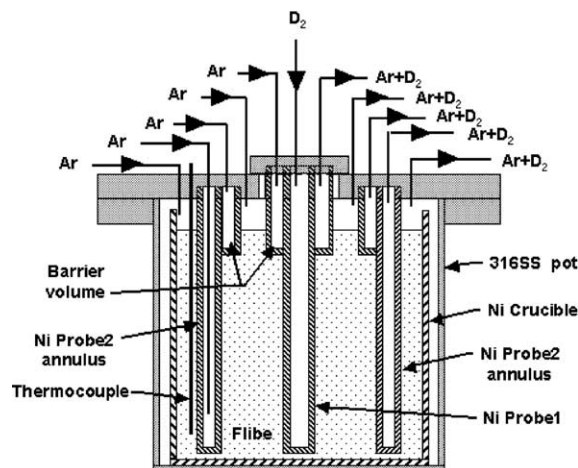


Fig. 1. Schematic illustration of cylindrically symmetric, permeation probe assembly.

nickel [19]. All the data were correlated based on model simulation calculations with the TMAP4 code [20] and the results were in good agreement with the observed experimental permeation behavior. Measured transient deuterium build-up data for probe-2 indicated that mixing of deuterium with Ar flow in the probe volume was the rate-limiting process for deuterium buildup and that the effect of deuterium diffusion in the probe-tube nickel walls was limited to about 1 min after the start of the transient.

### 3.2. Permeation measurements with Flibe

Several deuterium permeation experiments were made with the system at temperatures of 600 and 650 °C and with a deuterium pressure of around  $9.0 \times 10^4$  Pa in probe-1. Ar flow rates through probe-2, through the barrier volumes, and over the Flibe were varied in the different experiments to investigate the influence of purge gas flow rates on observed deuterium build-up transient behavior. Results are presented here for Ar purge gas flow-rates of 25 cc/min through probe-2 and over the Flibe and with 50 cc/min through the barriers.

Fig. 2 compares the results of deuterium permeation experiments at 600 °C with no Flibe in the system (Exp A) and with Flibe filling the assembly (Exp B). Probe-2 Ar flow rates were 25 cc/min for both experiments. For Exp A, measured  $D_2$  partial pressures in probe-2 (dash-dot line) are plotted relative to the left ordinate. The Exp A deuterium transient behavior reflects the condition with no Ar flow through the volume between the probes and the case when the flow through the inter-probe volume was changed to 100 cc/min. The transient deuterium behavior was well matched with TMAP4 model calculations, and derived permeability coefficients agreed with previous work [17,18]. For Exp B, measured  $D_2$  partial pressure data (right ordinate reference) are shown for probe-2 (solid line) and above the Flibe (dash line). Because the QMS was alternately switched to

analyze flow streams through probe-2 and above the Flibe, the plotted data show regions with no scatter. Two features of the Exp B data reflect the influence of Flibe on permeation. First, there is significant time delay in the probe-2  $D_2$  permeation signal and in the buildup of deuterium above the Flibe. Second, the maximum  $D_2$  partial pressures in probe-2 and above the salt are much less than those observed in Exp A. These results are due to the low solubility and slow diffusivity of  $D_2$  in Flibe.

TMAP-4 simulation calculations were used to evaluate the overall deuterium permeation rates in the Flibe/Ni/ $D_2$  system using previously reported transport data for these materials. These analyses showed that diffusion in Flibe was rate-determining for our experimental conditions. Therefore, for the two-probe Flibe experiments, the governing transport equation could be integrated in cylindrical coordinates giving the following analytical solution for the deuterium permeation flux,  $j$ ,

$$\frac{jb}{DKp_0} = \frac{1}{\ln(b/a)} - \sum_{n=1}^{\infty} \frac{2J_0(a\alpha_n)J_0(b\alpha_n) \exp(-\alpha_n^2 Dt)}{(J_0(b\alpha_n) - J_0(a\alpha_n))(J_0(b\alpha_n) + J_0(a\alpha_n))},$$

$$N_0(a\alpha_n)J_0(b\alpha_n) = N_0(b\alpha_n)J_0(a\alpha_n),$$

where  $D$  is diffusivity,  $K$  is solubility,  $p_0$  is pressure in probe-1,  $a$  and  $b$  are radii of probe surfaces bounding the Flibe,  $J_0$  and  $N_0$  are zeroth order Bessel functions of the first and second kind, respectively, and values of  $\alpha_n$  are determined by the second equation. Results from calculations with the above analytical expressions and with TMAP-4 showed good agreement in the initial breakthrough and buildup of the permeation flux with some deviation between calculated quantities at steady state times, most likely due to coordinate system calculation differences.

Results of the analytical fit (by adjustment of  $D$  and  $K$  values) to experimental data measured at 600 and 650 °C are shown in Figs. 3 and 4, respectively. We obtained close agreement between analytical fit and experimental data for the 600 °C experiment and reasonable agreement for the 650 °C experiment for times less than 4 h. Deviations in the 650 °C data comparison at times greater than 4 h may be related to: actual changes in probe-2 purge gas flow rate, possible inadequate model representation of Ar and  $D$  mixing in probe-2, and possible onset of thermal convection effects in the molten salt. However, values of  $D$  were determined by the build-up or breakthrough time and values of  $K$  were determined by the build-up rate, and they provided the following estimates of diffusion and solubility coefficients for deuterium in Flibe:  $D = 8.0 \times 10^{-10}$  m<sup>2</sup>/s and  $K = 3.1 \times 10^{-4}$  mol/m<sup>3</sup> Pa for 600 °C, and  $D = 3.0 \times 10^{-9}$  m<sup>2</sup>/s and  $K = 1.0 \times 10^{-4}$  mol/m<sup>3</sup> Pa for 650 °C.

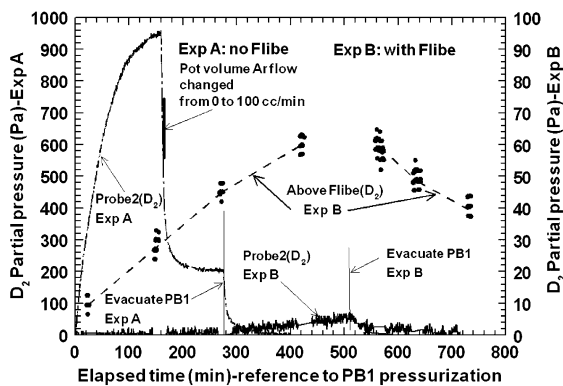


Fig. 2. Comparison of measured deuterium transport data for experiments at 600 °C with and without Flibe.

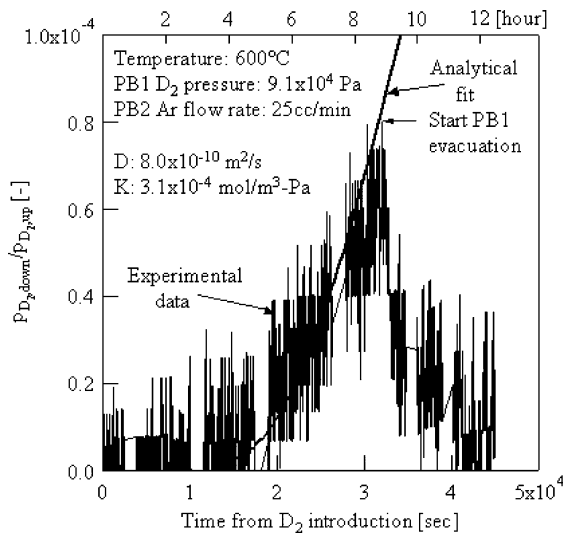


Fig. 3. Fit of an analytical transport solution expression to deuterium partial pressure data measured in probe-2 for Flibe at 600 °C.

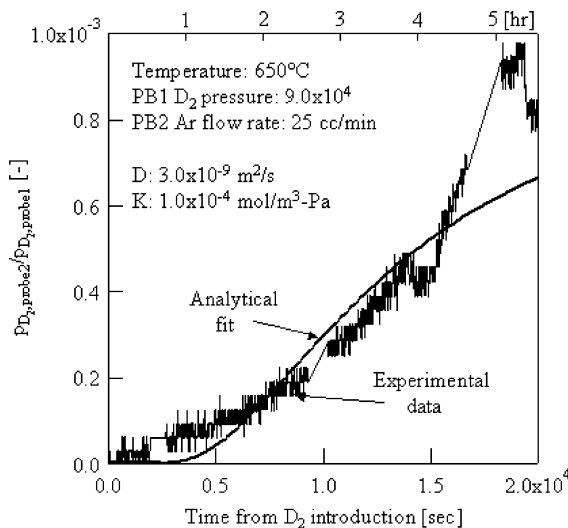


Fig. 4. Fit of an analytical transport solution expression to deuterium partial pressure data measured in probe-2 for Flibe at 650 °C.

#### 4. Discussion and conclusions

Diffusion coefficients derived from these experiments are compared to previously published data in Fig. 5. Our diffusion results are a little less than those reported by Oishi et al. [12] for  $T^+$  transport in molten Flibe, suggesting that deuterium was also diffusing as the  $D^+$  species in our experiments. Both of these results are

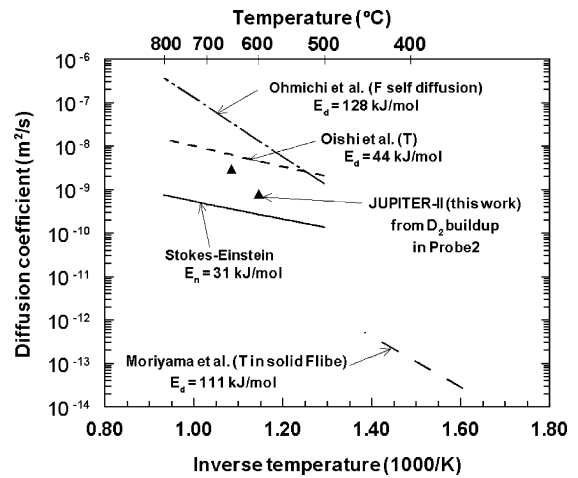


Fig. 5. Diffusion coefficients for Flibe.

somewhat greater than those derived from the viscosity using the Stokes–Einstein relation,  $D = kT/(6\pi R\eta)$ , assuming a particle radius,  $R$ , of 2 Å and a viscosity,  $\eta$ , reported by Cantor [21] for  $2LiF \cdot BeF_2$ . The diffusion activation energy for the Oishi et al. data is consistent with the viscosity data. However, a two-point fit to our diffusion coefficients (a dangerous approach with such limited data) yields a diffusion activation energy comparable to that for  $F^-$  self-diffusion. Such a result would suggest transport mechanisms similar to that postulated by Ohmichi et al. [22], namely ion-pair diffusion or exchange processes that break Be–F bonds.

Solubility coefficients derived from these experiments were comparable to those for DF in Flibe, as reported by Field and Shaffer [15], rather than to those for  $H_2$ ,  $D_2$ , reported by Malinauskas et al. [14]. These results suggest that the chemical potential of deuterium in the Flibe for the current experiments was greater than the chemical potential of  $D$  solute when the dominant species of deuterium in Flibe was  $D_2$ . This interpretation is consistent with previous experiments [7–11] in which a significant overpressure of hydrogen was required to promote exchange reactions with TF in the salt and facilitate transport of tritium in the Flibe as HT.

We conclude from these results that deuterium transport in the present experiments was mediated by the presence of a bond between  $D^+$  and  $F^-$  in the molten salt. This could be due to the presence of excess residual HF or free fluorine in the salt following the hydro-fluorination purification process, to ion-pair diffusion processes suggested by Ohmichi et al. [22], or to insufficient concentrations of deuterium in the salt. To better elucidate the mechanisms for hydrogen isotope transport in molten Flibe, future experiments should include systematic control of the hydrogen content and free fluorine content in the salt by suitable REDOX control

agents like Be and improved temperature control to minimize thermal convection effects.

### Acknowledgements

This work was supported partially by the US Department of Energy, Office of Sciences, and by the Japan–US joint research program, JUPITER-II, under the DOE Idaho Operations Contract DE-AC07-99ID13727.

### References

- [1] R.W. Moir et al., *Fus. Technol.* 19 (1991) 617.
- [2] A. Sagara et al., *Fus. Eng. Des.* 29 (1995) 51.
- [3] A. Sagara et al., *Fus. Technol.* 39 (2001) 753.
- [4] D.K. Sze et al., *Fus. Technol.* 39 (2001) 789.
- [5] D.A. Petti et al., *Fus. Sci. Technol.* 41 (2002) 807.
- [6] H. Moriyama et al., *J. Nucl. Mater.* 148 (1987) 211.
- [7] T. Terai et al., *Fus. Technol.* 39 (2001) 768.
- [8] A. Suzuki et al., *Fus. Eng. Des.* 39&40 (1998) 781.
- [9] A. Suzuki et al., *J. Nucl. Mater.* 258–263 (1998) 519.
- [10] A. Suzuki et al., *Fus. Technol.* 34 (1998) 526.
- [11] T. Terai et al., *Fus. Technol.* 30 (1996) 911.
- [12] J. Oishi et al., *Fus. Eng. Des.* 8 (1989) 317.
- [13] H. Moriyama et al., *J. Nucl. Mater.* 161 (1989) 197.
- [14] A.P. Malinauskas et al., *Ind. Eng. Chem. Fundam.* 13 (3) (1974) 242.
- [15] P.E. Field, J.H. Shaffer, *J. Phys. Chem.* 71 (10) (1967) 3218.
- [16] J.H. Shaffer, Preparation of and handling of salt mixtures for the molten salt reactor experiment, ORNL-4616, January 1971.
- [17] S. Fukada et al., *Fus. Eng. Des.* 61&62 (2002) 78.
- [18] S. Fukada et al., *Fus. Sci. Technol.* 44 (2003) 410.
- [19] W.E. Robertson, *Z. Metallkunde* 64 (1973) 436.
- [20] G.R. Longhurst et al., TMAP4 User's Manual, EGG-FSP-10315, 1998.
- [21] S. Cantor, Physical properties of molten-salt reactor fuel, coolant and flush salts, ORNL-TM-2316, August 1968.
- [22] T. Ohmichi et al., *J. Phys. Chem.* 80 (1976) 1628.